

# Simple Nanosecond to Minutes Transient Absorption Spectrophotometer

ALEKSANDR V. MIKHONIN, MARTA K. MAURER, CHAD E. REESE, and SANFORD A. ASHER\*

*Department of Chemistry, University of Pittsburgh, Pittsburgh, Pennsylvania 15260 (A.V.M., S.A.A.); Pennsylvania State University, 129K Smith Building, 3000 Ivyside Park, Altoona, Pennsylvania 16601-3760 (M.K.M.); and Mylan Pharmaceuticals, 3711 Collins Ferry Road, Morgantown, West Virginia 26505 (C.E.R.)*

We built a transient absorption spectrophotometer that can determine transient absorption spectral changes that occur at times as fast as ~200 ns and as slow as a minute. The transient absorption can be induced by a temperature-jump (T-jump) or by optical pumping from the deep ultraviolet (UV) to the infrared (IR) by use of single ns Nd:YAG laser pulses. Our use of a fiber-optic spectrometer coupled to a XeF flashlamp makes the collection of transient spectra easy and convenient in the spectral range from the near IR (1700 nm) down to the deep UV (200 nm), with high signal-to-noise (S/N) ratios. The spectral resolution is determined by the specific configuration of the fiber-optic spectrometer (grating groove density, fiber diameter, slit width) and varies between 0.3 and 10 nm. The utility of this spectrometer was demonstrated by measuring the rate at which a polymerized crystalline colloidal array (PCCA) of poly(N-isopropylacrylamide) nanogel particles optically switch light due to a T-jump induced by nanosecond 1.9  $\mu\text{m}$  laser pulses. In addition, we measured the rate of optical switching induced by a 3 ns 355 nm pump pulse in PCCA functionalized with azobenzene.

Index Headings: Transient absorption; Temperature jump; Pump probe; Optical switching; Volume-phase transition; Photonic crystals.

## INTRODUCTION

Many chemical and biochemical processes occur in the nanosecond, microsecond, and millisecond timescales. Examples include electron transfer and the relaxation of reactive species such as radicals and photochemically produced excited states,<sup>1–6</sup> protein folding,<sup>7–10</sup> RNA folding,<sup>11</sup> hydrogel volume-phase transitions,<sup>12–14</sup> and macromolecular self-assembly.<sup>15</sup> Specialized instruments are used to monitor these processes at these various timescales.

These instruments typically utilize optical spectroscopic techniques with high time resolution. Examples include transient visible and/or near-infrared (NIR) absorption spectrometers,<sup>1,16–24</sup> fluorescence spectrometers,<sup>25–34</sup> circular dichroism (CD) spectrometers,<sup>35–38</sup> IR spectrometers,<sup>18,24,39–42</sup> and Raman<sup>10,18,43,44</sup> spectrometers. Recently, these optical spectroscopic methods have been extended into the picosecond and femtosecond time regions.<sup>16,45–49</sup> Most of these spectroscopic instruments are complex, utilize rather specialized equipment, are home-built, and are not available commercially. In addition, many of these instruments are designed only for a particular application in a limited spectral region.

Transient absorption instruments are usually less complicated than other spectroscopic instruments. The transient absorption changes can be initialized using laser-induced T-jumps (when the IR pump beam is absorbed by solvent) or photochemically with the pump-beam-induced absorption changes occurring in the ultraviolet (UV), visible, or IR spectral regions depending on the sample. These transient changes can be monitored either at a single wavelength of interest or by recording the entire transmittance spectrum of the region of interest.

In the “single wavelength detection mode”, either a continuous wave (CW) or probe laser pulse at a certain wavelength can be used. Alternatively, a single wavelength can be selected from a “white light probe pulse” by a monochromator. Then, the transient absorption changes at the chosen wavelength can be detected by simple and inexpensive devices such as photomultiplier tubes (PMT) or photodiodes. The CW probe can be monitored kinetically with an oscilloscope, for example. The experimental convenience of single channel transient measurement is balanced by the necessity of avoiding confounding baseline changes.

More complete kinetic information can be obtained by simultaneously recording transient absorption spectra over larger spectral regions. This measurement requires a reliable pulsed “white light” source as well as a spectrometer coupled to a multichannel detector such as a photodiode array or charge-coupled device (CCD, ICCD) camera, etc.

Pulsed flashlamp(s) can be used to generate such a “white light” pulse. The modern commercially available lamps can cover the spectral range from UV to NIR (~160 to 2000 nm), providing relatively stable high intensity pulses. These pulsed lamps are, at present, limited to >100 ns time resolution.

In the work here we describe the construction of a simple UV–visible NIR transient absorption spectrophotometer built from simple, relatively inexpensive commercially available off-the-shelf equipment. This absorption spectrometer can also be easily reconfigured to operate as a transient fluorescence spectrometer or laser-induced breakdown (LIBS) spectrometer.

We initiate the transient absorption spectral changes by a nanosecond Nd:YAG laser either by using a temperature jump, which derives from absorption of a single IR laser pulse by the solvent, or we can initiate photochemistry by NIR, visible, or UV nanosecond light pulses. The spectrograph utilizes a XeF pulsed flashlamp as the transient white light source, which transmits through the sam-

Received 16 May 2005; accepted 29 September 2005.

\* Author to whom correspondence should be sent. E-mail: asher@pitt.edu.

**TABLE I.** Nd:YAG wavelengths easily obtained by harmonic generation and/or Raman shifting in H<sub>2</sub> gas available to pump a desired sample.

Nd:YAG harmonics	Fundamental	2nd harmonics	3rd harmonics	4th harmonics	5th harmonics
2nd Stokes		954 nm	503 nm	341.5 nm	258.5 nm
1st Stokes	1.9 $\mu\text{m}$ 2.2 mJ <sup>b</sup>	683 nm	416 nm	299 nm	233 nm
Direct output	1064 nm 100 mJ <sup>a</sup>	532 nm 65 mJ <sup>a</sup>	355 nm 32 mJ <sup>a</sup>	266 nm	213 nm
1st anti-Stokes	738 nm	436 nm	309 nm	240 nm	195.5 nm
2nd anti-Stokes	565 nm	369 nm	274 nm	218 nm	180.8 nm
3rd anti-Stokes	457 nm	320 nm	246 nm	200 nm	
4th anti-Stokes	384 nm	282 nm	223 nm	184.5	
5th anti-Stokes	331 nm	253 nm	204 nm 20 $\mu\text{J}$ <sup>a</sup>		

<sup>a</sup> All pulse energies were measured for a 100 mJ per pulse energy for the Nd:YAG fundamental at 100 Hz; the maximum fundamental pulse energy of Nd:YAG Infinity laser is 500 mJ.

<sup>b</sup> This value of 2.2 mJ/pulse was measured at  $\sim$ 50 mJ per pulse of the Nd:YAG fundamental at 90 Hz.

ple and is then coupled into a miniature fiber-optic spectrograph. The spectrum of the transmitted light is monitored between 200–1700 nm (Ocean Optics USB2000: 200–1100 nm) by coupling the spectrograph to a multi-channel detector. As discussed below, this apparatus can be utilized to study a large variety of chemical and biochemical processes.

## INSTRUMENTATION

**Description of Transient Absorption Setup.** The transient absorption of the sample can be initiated conveniently by the 1064 nm fundamental output of a Coherent Radiation Infinity Nd:YAG laser or by its harmonics, and/or by its Raman shifted lines in hydrogen gas.<sup>10,13,33,42,50–63</sup> The wavelengths easily available for pumping are shown in Table I. Table I also shows the pulse energies (where available) that can be generated using 100 mJ fundamental pulses at a 100 Hz repetition rate of the Nd:YAG Infinity laser (unless stated differently). It should be noted that pulse energies given in Table I are not the maximum powers that can be generated, since the Nd:YAG Infinity laser can provide up to 500 mJ fundamental pulses.

The Nd:YAG fundamental at 1064 nm can be used directly to excite a temperature jump by exciting overtones of solvents. However, we generally utilize the easily generated 1.9  $\mu\text{m}$  excitation, which is strongly absorbed by both water and D<sub>2</sub>O. This excitation wavelength is efficiently generated by Stokes Raman shifting the 1064 nm YAG fundamental in high-pressure ( $\sim$ 1000 psi) hydrogen gas. The YAG harmonics at 532 nm in the green, at 355 in the near UV, and at 266 nm in the mid-UV, as well as the fifth harmonic at 213 nm can also be generated by the YAG laser. In addition, there are numerous additional Raman shifted lines that can be used to excite electronic absorption bands throughout the UV and visible spectral regions (Table I).

As shown in Fig. 1 the output of the Nd:YAG laser, which may have been Raman shifted, was filtered by using a Pellin Broca prism and then diffusely focused through a thin sample cell ( $\sim$ 1 mm) at an angle  $\sim$ 10° from the normal. The output of the polychromatic light from a XeF IBH5000 flashlamp (HORIBA Jobin Yvon IBH Ltd; Glasgow, UK) was incident normal to the sample cell and focused to transmit through the volume excited by the YAG pump beam. We normally operate the XeF IBH5000 flashlamp between 750 and 850 volts.

The timing between the pump and probe beams was controlled electronically. The firing of the Nd:YAG laser initiates a TTL pulse that can be delayed from a few nanoseconds to 6 ms times. This TTL pulse initiates firing of the XeF flashlamp at the desired delay time. The minimum time resolution is limited to  $\sim$ 200–300 ns because of the XeF flashlamp  $\geq$ 120 ns temporal pulse width and because of the  $\sim$ 50 to 200 ns jitter between the YAG pulse and XeF lamp pulse. The latter jitter occurs because the external lamp trigger does not directly control the instant the XeF flashlamp fires; rather, it begins the sequence of events that ultimately results in the XeF lamp output. We find that the magnitude of the jitter delay can be partially controlled by the voltage applied to the XeF flashlamp. The jitter delay is decreased by increasing the lamp voltage.

We measured transmission of individual XeF flashlamp pulses through the sample by using an Ocean Optics USB2000 Miniature Fiber Optic Spectrometer. The fiber contains a collection lens that focuses the light into a small spectrograph, which disperses the light over the

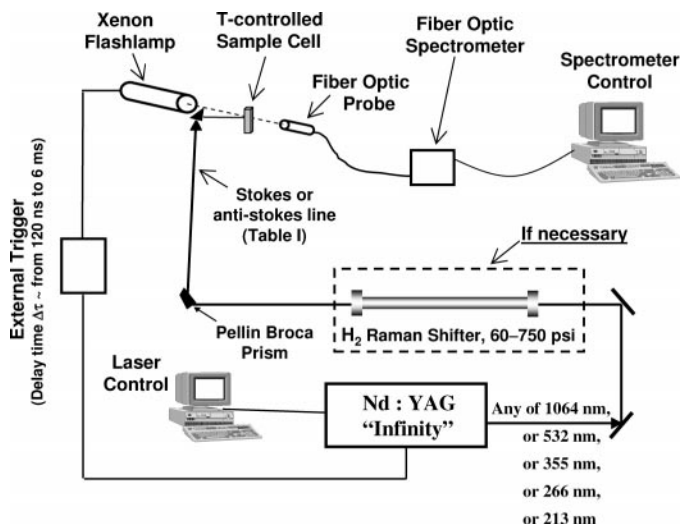


**FIG. 1.** Experimental setup for transient absorption measurements initiated either photochemically or by laser-induced temperature jump.

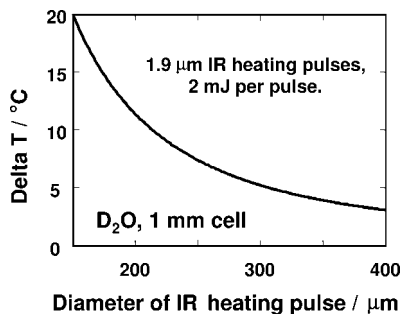


FIG. 2. Estimated T-jump values in D<sub>2</sub>O (1 mm cell) for different diameters of 1.9  $\mu\text{m}$  IR heating pulses with an energy of 2 mJ per pulse. We used D<sub>2</sub>O absorbance of 6  $\text{cm}^{-1}$  and a heat capacity of 3.8 J/g.

face of a photodiode array detector. This USB2000 spectrograph specifically covers the spectral range between 200 and 1100 nm with a resolution from 0.3 to 9 nm depending on its particular configuration. Use of a NIR512 Ocean Optics Fiber Optic Spectrometer would allow us to extend the measured spectral region up to 1700 nm.

The spectrometer separately measures the sample transmission at the appropriate delay of the XeF flash-lamp pulse in the presence and absence of the pump beam. In the case of UV or visible excitation pulse, a filter was used to reject the pump beam intensity from scattering into the collection fiber optic. The spectrum measured in the absence of the pump pulse was obtained by simply blocking the pump pulse.

A dark noise spectrum was also measured under identical conditions where the pump and XeF lamp pulses were both blocked. The dark noise spectrum was subtracted from transmission spectra measured both in the presence and absence of the pump pulse. The transient transmission spectrum at the defined delay time is calculated as the ratio of these dark-noise-corrected spectra.

**Absorbance Conditions for Laser Pump Beam with Respect to “White” XeF Lamp Probe Beam.** We controlled the concentrations of our transient samples such that only modest attenuation of the pump beam occurred as it passed through the sample such that the photochemistry or T-jump was relatively uniform along the sample depth. For the T-jump, where the excitation was independently absorbed by the solvent, we were able to independently adjust the analyte concentration to maximize the absorption measurement signal-to-noise (S/N) ratio.

These considerations determine the sample concentration, sample thickness, and choice of solvent. For the T-jump measurements we optimized the D<sub>2</sub>O/water concentration to set the required NIR absorption.

**T-jump Measurements.** The output of the YAG laser fundamental at 1064 nm YAG ( $\sim 50$  mJ) was Raman shifted to the first H<sub>2</sub> Stokes harmonic at 1.9  $\mu\text{m}$  by using a 1 m Raman shifter (Light Age Inc., 1000 psi H<sub>2</sub>) to obtain a  $\sim 2$  mJ pulse energy. This 1.9  $\mu\text{m}$  excitation beam is strongly absorbed by water and/or D<sub>2</sub>O combination tones/overtone and the energy is thermalized within picoseconds by vibrational relaxation.<sup>7</sup>

Pure water shows a 1.907  $\mu\text{m}$  absorbance of  $\sim 40/\text{cm}$ ,<sup>10</sup> which requires using pure water samples of  $< 100$   $\mu\text{m}$  sample thicknesses. Alternatively, one can dilute H<sub>2</sub>O

## Optical switching from PNIPAM CCA

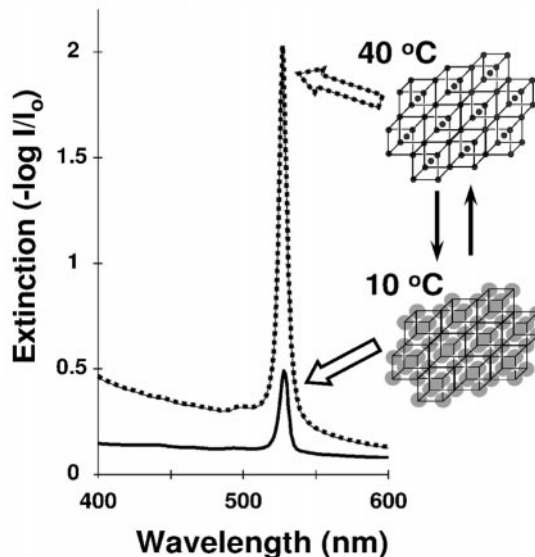


FIG. 3. Schematic diagram of the volume-phase transition of PNIPAM particles in CCA. The shrunken particles at  $T > 33$   $^{\circ}\text{C}$  diffract light more efficiently than the swollen ones at  $T < 33$   $^{\circ}\text{C}$ .

with D<sub>2</sub>O, which absorbs much less,  $\sim 6/\text{cm}$ , and use the appropriate D<sub>2</sub>O/water mixtures for thicker samples. It should be mentioned that we utilize 6  $\text{cm}^{-1}$  D<sub>2</sub>O absorbance measured using the Cary 5000 UV-VIS NIR Spectrophotometer, which is significantly lower than reported earlier by other groups.<sup>42,50</sup>

The value of the T-jump occurring in the polymerized poly-N-isopropylacrylamide hydrogel particles (PNIPAM) in D<sub>2</sub>O in a 1 mm sample cell after the arrival of a single 1.9  $\mu\text{m}$  IR pulse is a function of IR beam diameter and can be estimated from Fig. 2. We chose to focus the 2 mJ 1.9  $\mu\text{m}$  laser pulses to a  $\sim 300$   $\mu\text{m}$  diameter, since such a relatively large diameter simplifies the probe beam focusing into the heated volume and allows us to obtain acceptable T-jumps of  $\Delta T \approx 5$ –6  $^{\circ}\text{C}$ .

We verified the magnitude of the T-jump by measuring the pump beam energy before and after the sample. We also measured the steady-state spectra at different temperatures to compare them to the spectra recorded after the arrival of the IR heating pulse at essentially infinite delay times. Measurements in the absence of the pump pulse demonstrated that negligible sample heating occurs from the XeF lamp pulse.

**355 nm Excitation Measurements.** In this mode, the apparatus pumps a sample with 3 ns pulses at 355 nm (3rd harmonics of Nd:YAG laser) at any desired pulse energy up to  $\sim 150$  mJ and at any desired frequency between 0.1 to 100 Hz. We delayed the XeF flashlamp with respect to the 355 nm laser pulse exactly the same way as described above for our instrument in T-jump mode. Analogously to the T-jump mode, we recorded the transient absorbance/transmittance changes using an Ocean Optics USB2000 Miniature Fiber Optic Spectrometer to monitor the spectral changes between 200 and 1100 nm.

## RESULTS

**Monitoring the Rate of PNIPAM Optical Switching.** We examined the rate of the volume-phase transition

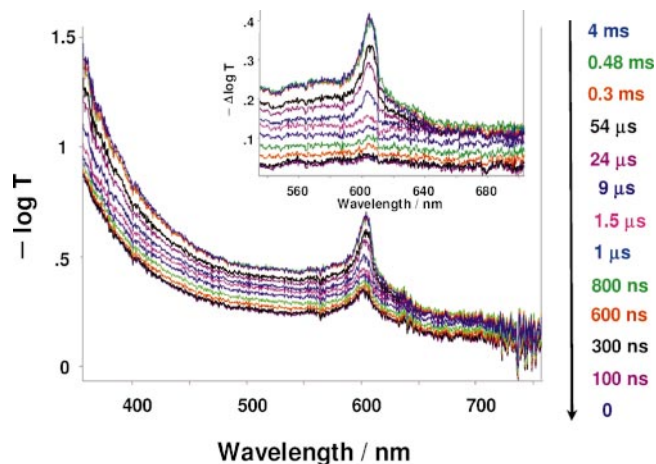


FIG. 4. Extinction time evolution for a PNIPAM PCCA sample after a T-jump from  $T = 30\text{ }^{\circ}\text{C}$  to  $T = 35\text{ }^{\circ}\text{C}$ . The fcc (111) diffraction peak maximum occurs at 605 nm. Spectra were measured at the times listed, subsequent to the T-jump. The inset displays difference spectra that highlight the T-jump spectral changes.

from a face-centered cubic array of PNIPAM particles polymerized in a hydrogel (Fig. 3). PNIPAM particles have been demonstrated to undergo a temperature-induced volume-phase transition.<sup>65</sup> At temperatures below the lower critical solution temperature ( $\sim 33\text{ }^{\circ}\text{C}$ ) this polymer is highly swollen. However, an increase in temperature expels water from the polymer network and the particle volume dramatically shrinks. This volume-phase transition can be monitored by changes in the light scattering of these particles in a crystalline colloidal array (CCA) (Fig. 3) due to the resulting increase in the refractive index of these particles.<sup>13,14,65</sup>

We polymerized a face-centered cubic CCA of PNIPAM nanogel particles<sup>65</sup> into a macroscopic acrylamide/bisacrylamide hydrogel using a procedure described earlier.<sup>66</sup> This polymerized CCA (PCCA) diffracts light in the visible spectral region due to the spacing between particles.<sup>65</sup> The individual PNIPAM nanogel particles still are able to undergo their individual volume-phase transitions.<sup>67</sup>

The acrylamide/bisacrylamide hydrogel constrains the centers of mass of the nanogel PNIPAM particles within the face-centered cubic (fcc) lattice and keeps the spacing between these centers of mass approximately constant.<sup>13,66</sup> Thus, for this sample the volume-phase transition induced by a temperature increase will result in a strong increase in the diffraction peak intensity due to shrinkage of the individual PNIPAM particles in a polymer network, without a change in wavelength.<sup>13,65</sup> The increased diffraction efficiency will result from the shrinkage of the particles, which gives them a larger dielectric constant. This results in an increase in the periodic modulation of the PCCA dielectric constant. We expect the diffraction switching will occur in the nanosecond time domain.<sup>13,14</sup>

For the PNIPAM PCCA we examined a sample of 1 mm thickness containing polymerized particles (spheres) in pure  $\text{D}_2\text{O}$  solution (assuming a face-centered cubic (fcc) lattice).<sup>13,65</sup> In this case about 75% of the  $1.9\text{ }\mu\text{m}$  heating pulse energy was absorbed in the 1 mm sample thickness.

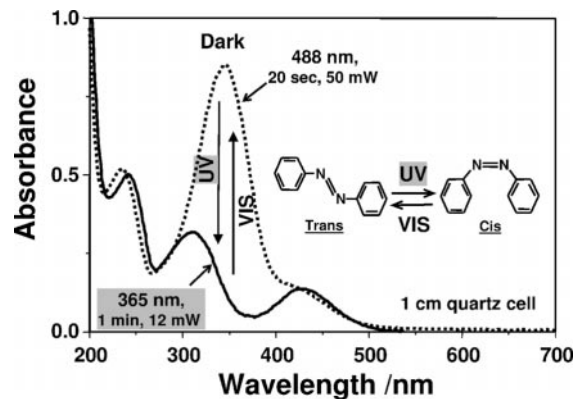


FIG. 5. Typical photochemistry of free azobenzene and its derivatives in solution. UV radiation induces the *cis* form, while VIS radiation induces the *trans* form. Both these transitions are reversible.

Figure 4, which is adapted from Reese et al.,<sup>13</sup> shows the ability of our instrument to detect the transient diffraction changes in PNIPAM-based PCCA initiated by a 3 ns T-jump from 30 to 35  $^{\circ}\text{C}$ . This figure shows the evolution of extinction ( $-\log T$ ) as a function of delay time subsequent to the  $1.9\text{ }\mu\text{m}$  heating pulse. The inset in Fig. 4 shows the difference spectra between the kinetically measured spectra and the initial “steady-state” absorption spectrum at  $+30\text{ }^{\circ}\text{C}$ . The extinction increases with increasing delay times at all wavelengths, with the largest increase for the 111-plane diffraction peak ( $\lambda_{111} \sim 605\text{ nm}$ ). The extinction at wavelengths  $>\lambda_{111}$  increases less than that at wavelengths  $<\lambda_{111}$ .

At  $\lambda \leq \lambda_{111}$  the extinction kinetics show at least three components with characteristic times of  $\sim 900\text{ ns}$ ,  $\sim 20\text{ }\mu\text{s}$ , and  $\sim 140\text{ }\mu\text{s}$ , respectively. The fastest and “middle” components are responsible for  $\sim 25\%$  of the entire kinetic changes each, while the slowest component accounts for  $\sim 50\%$  of the transient absorption changes. At  $\lambda < \lambda_{111}$  there is a slight increase in the slow component contribution compared to that at  $\lambda = \lambda_{111}$ .

This multi-exponential shrinking may result from differences in composition of the interior versus the periphery of these nanogel particles.<sup>14,68–74</sup> The periphery of these particles may have fewer cross-links and be more hydrophilic than the core. The osmotic pressure that actuates the shrinkage would then be spatially inhomogeneous, which could lead to complex kinetics.

**Monitoring 355 nm Pump *Trans*–*Cis* Diffraction Kinetics in Azobenzene PCCA.** It is well known that the azobenzene derivatives normally exist in their *trans* ground state conformations at room temperature in the dark.<sup>12,75,76</sup> This *trans* conformation shows a strong absorption maximum at  $\sim 340\text{ nm}$ , which results from its  $\pi \rightarrow \pi^*$  ( $S_0 \rightarrow S_2$ ) transition.<sup>77–79</sup> Upon excitation with UV light, the *trans* azobenzene derivative(s) isomerizes within picoseconds to the *cis* form.<sup>12,47,77–83</sup> This *trans*-to-*cis* transformation is accompanied by a strong decrease in the  $\sim 340\text{ nm}$  absorption (Fig. 5). Many azobenzene derivatives show a large barrier to isomerization in the ground state. Thus, if the *cis* state were formed it could remain for weeks until it thermalized over the barrier to *trans*.<sup>12</sup>

The *cis*-azobenzene derivatives show an absorption band at  $\sim 435\text{ nm}$ , which results from its  $n \rightarrow \pi^*$  ( $S_0 \rightarrow$

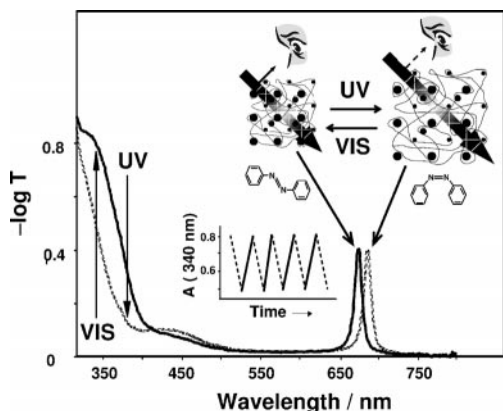


FIG. 6. Schematic diagram of the volume-phase transition in PCCA functionalized by covalently attached azobenzene. UV radiation ultimately causes the hydrogel network to swell, which can be monitored by the up-shifts (red-shifts) of the diffraction peak from the (111) plane. Visible radiation causes the polymer network to shrink and restores the original diffraction.

$S_1$ ) transition.<sup>77,84</sup> Excitation of the *cis* derivative(s) within this transition with visible light induces a *cis*-to-*trans* transition (Fig. 5).<sup>12,77,84</sup> For our azobenzene derivatives the *trans*-*cis* and *cis*-*trans* transitions were completely reversible upon sequential UV and visible radiation (Fig. 5).

A PCCA with covalently attached azobenzene was shown to undergo reversible transmission changes upon sequential UV and VIS light irradiation (Fig. 6).<sup>12</sup> The formation of the *cis*-azobenzene derivative attached to the hydrogel of the PCCA causes the hydrogel to swell and to red-shift the (111) plane diffraction maximum from  $\sim 445$  nm to  $\sim 460$  nm for that particular PCCA.<sup>12</sup> In contrast, visible irradiation causes the azobenzene to switch back to its *trans* form, causing the hydrogel to shrink and restore its original diffraction maximum at  $\sim 445$  nm.<sup>12</sup>

We measured transient absorption of the PCCA with covalently attached azobenzene by using the third harmonics of a Nd:YAG laser (355 nm). We used the sam-

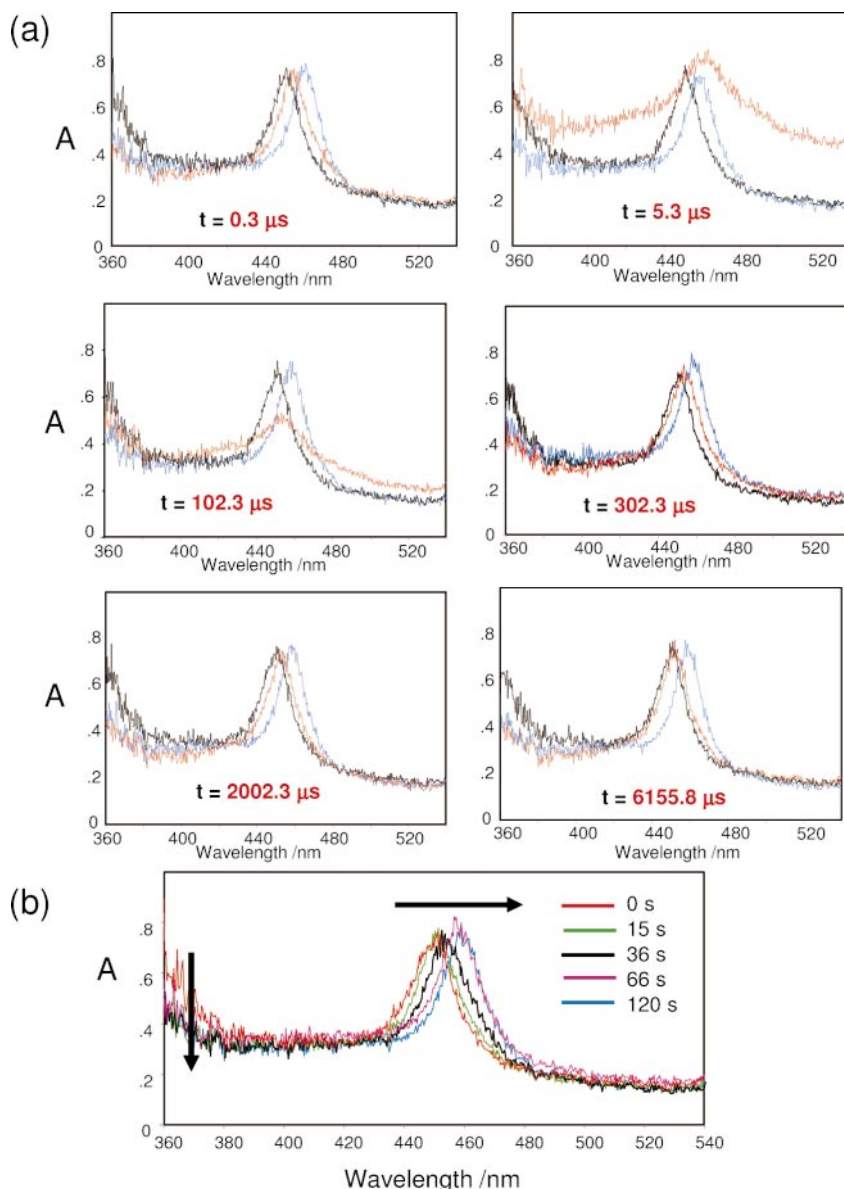


FIG. 7. (a) PCCA in dark (black), at the indicated time subsequent to excitation by one 3-ns 355-nm pulse (red), and after 1 min (blue). (b) Absorption spectral changes in the second time regime.

ples of 0.2 mm thickness and with azobenzene concentrations of 4.5 mM as described in detail elsewhere.<sup>12</sup>

Figure 7, which is adapted from Kamenjicki et al.,<sup>12</sup> shows the time evolution of the diffraction from a PCCA with attached azobenzene (initially in the *trans* conformation) as a function of delay time between the 355 nm pump pulse and XeF lamp probe pulse. The complicated behavior of the photochemical response of PCCA with attached azobenzene is discussed in detail elsewhere.<sup>12</sup> Briefly, azobenzene undergoes a fast subnanosecond *trans*-to-*cis* transition,<sup>47,78–83</sup> which starts the sequence of events in the PCCA, which occur at different timescales from nanoseconds to seconds, and finally results in the shift of the (111) plane diffraction peak from ~445 to ~460 nm for this particular PCCA.<sup>12</sup> In addition, we observe a fast (within the 300 ns deadtime of the instrument) absorbance decrease at ~360 nm due to conversion of azobenzene to its *cis* form. This is consistent with azobenzene photoisomerization studies that report picosecond photoisomerization.<sup>47,78–83</sup>

Thus, our transient absorption instrument is able to monitor the kinetics between 300 ns and minute time scales and can serve as an important tool for studying a variety of chemical and biochemical processes as discussed above.

## CONCLUSION

We have developed a powerful, simple, and convenient instrument that allows us to monitor fast and slow transient absorption/transmission changes in the time range from ~300 ns to minutes. This instrument can be used for temperature-jump studies (utilizing NIR heating pulses) as well as for photochemical excitation studies with excitation from the deep UV to visible using the harmonics of the Nd:YAG laser as well as Stokes and/or anti-Stokes harmonics in H<sub>2</sub> gas (Table I). The absorption/transmission changes can be monitored in the range from 200 to 1700 nm.

## ACKNOWLEDGMENTS

The authors thank Dr. Igor Lednev as well as NIH grant 8 RO1 EB002053021 for financial support.

1. M. M. Alam, A. Watanabe, and O. Ito, *J. Photochem. Photobiol. A* **104**, 59 (1997).
2. D. Wang, R. Mendelsohn, E. Galoppini, P. G. Hoertz, R. A. Carlisle, and G. J. Meyer, *J. Phys. Chem. B* **108**, 16642 (2004).
3. M. Sakamoto, X. Cai, M. Hara, S. Tojo, M. Fujitsuka, and T. Majima, *J. Phys. Chem. A* **108**, 8147 (2004).
4. S. Tanaka, C. Kato, K. Horie, and H.-O. Hamaguchi, *Chem. Phys. Lett.* **381**, 385 (2003).
5. E. A. Weiss, M. A. Rätner, and M. R. Wasielewski, *J. Phys. Chem. A* **107**, 3639 (2003).
6. L. X. Chen, G. Jennings, T. Liu, D. J. Gosztola, J. P. Hessler, D. V. Scaltrito, and G. J. Meyer, *J. Am. Chem. Soc.* **124**, 10861 (2002).
7. C. M. Phillips, Y. Mizutani, and R. M. Hochstrasser, *Proc. Natl. Acad. Sci. USA* **92**, 7292 (1995).
8. R. B. Dyer, F. Gai, W. H. Woodruff, R. Gilmanshin, and R. H. Callender, *Acc. Chem. Res.* **31**, 709 (1998).
9. M. Gruebele, J. Sabelko, R. Ballew, and J. Ervin, *Acc. Chem. Res.* **31**, 699 (1998).
10. I. K. Lednev, A. S. Karnoup, M. C. Sparrow, and S. A. Asher, *J. Am. Chem. Soc.* **121**, 8074 (1999).
11. A. P. Williams, C. E. Longfellow, S. M. Freier, R. Kierzek, and D. H. Turner, *Biochemistry* **28**, 4283 (1989).
12. M. Kamenjicki, I. K. Lednev, A. Mikhonin, R. Kesavamoorthy, and S. A. Asher, *Adv. Funct. Materials* **13**, 774 (2003).
13. C. E. Reese, A. V. Mikhonin, M. Kamenjicki, A. Tikhonov, and S. A. Asher, *J. Am. Chem. Soc.* **126**, 1493 (2004).
14. J. Wang, D. Gan, L. A. Lyon, and M. A. El-Sayed, *J. Am. Chem. Soc.* **123**, 11284 (2001).
15. A. Pandit, H. Ma, I. H. M. van Stokkum, M. Gruebele, and R. van Grondelle, *Biochemistry* **41**, 15115 (2002).
16. R. Katoh, A. Furube, A. V. Barzykin, H. Arakawa, and M. Tachiya, *Coordination Chem. Rev.* **248**, 1195 (2004).
17. T. Yoshihara, R. Katoh, A. Furube, Y. Tamaki, M. Murai, K. Hara, S. Murata, H. Arakawa, and M. Tachiya, *J. Phys. Chem. B* **108**, 3817 (2004).
18. J. Dyer, W. J. Blau, C. G. Coates, C. M. Creely, J. D. Gavey, M. W. George, D. C. Grills, S. Hudson, J. M. Kelly, P. Matousek, J. J. McGarvey, J. McMaster, A. W. Parker, M. Towrie, and J. A. Weinstein, *Photochem. Photobiol. Sci.* **2**, 542 (2003).
19. A. Matsumoto, K. Maeda, and T. Arai, *J. Phys. Chem. A* **107**, 10039 (2003).
20. A. Banderini, S. Sottini, and C. Viappiani, *Rev. Sci. Instrum.* **75**, 2257 (2004).
21. H. Zhang, Y. Zhou, M. Zhang, T. Shen, J. Xiang, and J. Feng, *J. Colloid Interface Sci.* **263**, 669 (2003).
22. N. K. Shrestha, E. J. Yagi, Y. Takatori, A. Kawai, Y. Kajii, K. Shibuya, and K. Obi, *J. Photochem. Photobiol. A* **116**, 179 (1998).
23. J. Jasny, J. Sepit, J. Karpiuk, and J. Gilewski, *Rev. Sci. Instrum.* **65**, 3646 (1994).
24. S. Boyde, G. F. Strouse, W. E. Jones, Jr., and T. J. Meyer, *J. Am. Chem. Soc.* **111**, 7448 (1989).
25. A. M. Ramos, E. H. A. Beckers, T. Offermans, S. C. J. Meskers, and R. A. J. Janssen, *J. Phys. Chem. A* **108**, 8201 (2004).
26. G. Grabner, K. Rechthaler, and G. Koehler, *J. Phys. Chem. A* **102**, 689 (1998).
27. B. Bangar Raju and S. M. B. Costa, *Phys. Chem. Chem. Phys.* **1**, 5029 (1999).
28. J. M. Calo, R. C. Axtmann, and R. G. Persing, *Rev. Sci. Instrum.* **41**, 1639 (1970).
29. C. L. Bashford, *Spectrophotometry. Spectrofluorometry* (2nd Edition), 283 (2000).
30. R. M. Ballew, J. Sabelko, C. Reiner, and M. Gruebele, *Rev. Sci. Instrum.* **67**, 3694 (1996).
31. J. Vecer, A. A. Kowalczyk, L. Davenport, and R. E. Dale, *Rev. Sci. Instrum.* **64**, 3413 (1993).
32. U. Alexiev, I. Rimke, and T. Pohlmann, *J. Mol. Biol.* **328**, 705 (2003).
33. U. Panne, C. Dicke, R. Duesing, R. Niessner, and G. Bidoglio, *Appl. Spectrosc.* **54**, 536 (2000).
34. R. Rigler, C. R. Rabl, and T. M. Jovin, *Rev. Sci. Instrum.* **45**, 580 (1974).
35. S. Wenzel and V. Buss, *Rev. Sci. Instrum.* **68**, 18868 (1997).
36. D. R. Bobbitt, *Techniques Instrum. Anal. Chem.* **14**, 15 (1994).
37. R. A. Goldbeck and D. S. Kliger, *Spectroscopy* (Duluth, MN, United States) **7**, 17–18, 20–24, 26, 28–29 (1992).
38. J. W. Lewis, R. F. Tilton, C. M. Einterz, S. J. Milder, I. D. Kuntz, and D. S. Kliger, *J. Phys. Chem.* **89**, 289 (1985).
39. A. Seilmeier, S. Hanna, V. A. Shalygin, D. A. Firsov, L. E. Vorobjev, V. M. Ustinov, and A. E. Zhukov, *Intl. J. Nanosci.* **2**, 445 (2003).
40. S. Williams, T. P. Causgrove, R. Gilmanshin, K. S. Fang, R. H. Callender, W. H. Woodruff, and R. B. Dyer, *Biochemistry* **35**, 691 (1996).
41. T. P. Causgrove and R. B. Dyer, *Biochemistry* **32**, 11985 (1993).
42. H. Ma, J. Ervin, and M. Gruebele, *Rev. Sci. Instrum.* **75**, 486 (2004).
43. G. Buntinx, O. Poizat, and N. Leygue, *J. Phys. Chem.* **99**, 2343 (1995).
44. E. W. Finsden and M. R. Ondrias, *Appl. Spectrosc.* **42**, 445 (1988).
45. G. Ramakrishna, A. K. Singh, D. K. Palit, and H. N. Ghosh, *J. Phys. Chem. B* **108**, 1701 (2004).
46. M. Towrie, D. C. Grills, J. Dyer, J. A. Weinstein, P. Matousek, R. Barton, P. D. Bailey, N. Subramaniam, W. M. Kwok, C. Ma, D. Phillips, A. W. Parker, and M. W. George, *Appl. Spectrosc.* **57**, 367 (2003).
47. I. K. Lednev, T. Q. Ye, P. Matousek, M. Towrie, P. Fogg, F. V. R. Neuwahl, S. Umaphathy, R. E. Hester, and J. N. Moore, *Chem. Phys. Lett.* **290**, 68 (1998).

48. I. V. Rubtsov, T. Zhang, and K. Yoshihara, *Bunko Kenkyu* **49**, 292 (2000).
49. S. M. Arrivo, V. D. Kleiman, T. P. Dougherty, and E. J. Heilweil, *Opt. Lett.* **22**, 1488 (1997).
50. J. Wang and M. A. El-Sayed, *Biophys. J.* **76**, 2777 (1999).
51. S. Ameen, *Rev. Sci. Instrum.* **46**, 1209 (1975).
52. R. W. Minck, R. W. Terhune, and W. G. Rado, *Appl. Phys. Lett.* **3**, 181 (1963).
53. D. P. Gerrity, L. D. Ziegler, P. B. Kelly, R. A. Desiderio, and B. Hudson, *J. Chem. Phys.* **83**, 3209 (1985).
54. B. S. Hudson and L. C. Mayne, *Methods Enzymol.* **130**, 331 (1986).
55. S. Wada, A. Kasai, and H. Tashiro, *Opt. Commun.* **88**, 146 (1992).
56. A. D. Papayannis, G. N. Tsirikas, and A. A. Serafetinides, *Appl. Phys. B* **67**, 563 (1998).
57. S. Tzortzakis, G. Tsaknakis, A. Papayannis, and A. A. Serafetinides, *Appl. Phys. B* **79**, 71 (2004).
58. J. A. Paisner and R. S. Hargrove, Proceedings of the Technical Program-Electro-Optics/Laser Conference & Exposition, 112 (1979).
59. Z. Chu, U. N. Singh, and T. D. Wilkerson, *Appl. Opt.* **30**, 4350 (1991).
60. V. Simeonov, V. Mitev, H. Van Den Bergh, and B. Calpini, *Appl. Opt.* **37**, 7112 (1998).
61. L. De Schoulepnikoff, V. Mitev, V. Simeonov, B. Calpini, and H. Van Den Bergh, *Appl. Opt.* **36**, 5026 (1997).
62. K. Sentrayan, A. Michael, and V. Kushawaha, *Appl. Phys. B* **62**, 479 (1996).
63. J. C. White, *Topics Appl. Phys.* **59**, 115 (1987).
64. M. Heskins, *J. Macromol. Sci., Chem.* **A2**, 1441 (1968).
65. J. M. Weissman, H. B. Sunkara, A. S. Tse, and S. A. Asher, *Science (Washington, D.C.)* **274**, 959 (1996).
66. S. A. Asher, J. Holtz, L. Liu, and Z. Wu, *J. Am. Chem. Soc.* **116**, 4997 (1994).
67. S. A. Asher, J. M. Weissman, and H. B. Sunkara, in *PCT Int. Appl.* (University of Pittsburgh of the Commonwealth System of Higher Education, Pittsburgh, Pennsylvania, Pa, 1998), p. 40.
68. X. Wu, R. H. Pelton, A. E. Hamielec, D. R. Woods, and W. McPhee, *Colloid Polym. Sci.* **272**, 467 (1994).
69. C. Wu, *Macromolecules* **30**, 574 (1997).
70. C. Wu, *Polymer* **39**, 4609 (1998).
71. A. Guillermo, J. P. C. Addad, J. P. Bazile, D. Duracher, A. Elaissari, and C. Pichot, *J. Polym. Sci., Part B: Polym. Phys.* **38**, 889 (2000).
72. D. Duracher, A. Elaissari, and C. Pichot, *Macromol. Symp.* **150**, 305 (2000).
73. T. Gilanyi, I. Varga, R. Meszaros, G. Filipcsei, and M. Zrinyi, *Phys. Chem. Chem. Phys.* **2**, 1973 (2000).
74. C. D. Jones and L. A. Lyon, *Macromolecules* **33**, 8301 (2000).
75. S. Yamashita, H. Ono, and O. Toyama, *Bull. Chem. Soc. Jpn.* **35**, 1849 (1962).
76. G. S. Hartley, *Nature (London)* **140**, 281 (1937).
77. G. Zimmerman, L.-Y. Chow, and U.-J. Paik, *J. Am. Chem. Soc.* **80**, 3528 (1958).
78. I. K. Lednev, T.-Q. Ye, R. E. Hester, and J. N. Moore, *J. Phys. Chem.* **100**, 13338 (1996).
79. I. K. Lednev, T.-Q. Ye, L. C. Abbott, R. E. Hester, and J. N. Moore, *J. Phys. Chem. A* **102**, 9161 (1998).
80. E. Chen, J. R. Kumita, G. A. Woolley, and D. S. Kliger, *J. Am. Chem. Soc.* **125**, 12443 (2003).
81. Y. Hirose, H. Yui, and T. Sawada, *J. Phys. Chem. A* **106**, 3067 (2002).
82. H. Satzger, S. Sporlein, C. Root, J. Wachtveitl, W. Zinth, and P. Gilch, *Chem. Phys. Lett.* **372**, 216 (2003).
83. H. Satzger, C. Root, and M. Braun, *J. Phys. Chem. A* **108**, 6265 (2004).
84. S. Malkin and E. Fischer, *J. Phys. Chem.* **66**, 2482 (1962).